

FINE-STRUCTURE EXCITATION OF C⁺ AND Si⁺ BY ATOMIC HYDROGEN

ĠIRTS BARINOVŠ AND MARC C. VAN HEMERT

Theoretical Chemistry Group, Leiden Institute of Chemistry, Leiden University, P.O. Box 9502, 2300 RA Leiden, Netherlands

AND

ROMAN KREMS AND ALEXANDER DALGARNO

Institute for Theoretical Atomic, Molecular and Optical Physics, Harvard-Smithsonian Center for Astrophysics,
60 Garden Street, Cambridge, MA 02138

Received 2004 September 17; accepted 2004 October 18

ABSTRACT

We present calculations of cross sections for fine-structure excitation in collisions of carbon and silicon ions in the ²P state with atomic hydrogen in the ground state. The results are based on accurate calculations of CH⁺ and SiH⁺ molecular potentials, including electronic core correlation and relativistic effects. We find that the energy dependence of the excitation cross sections is largely determined by shape resonances. Our work improves on the results of previous calculations with less accurate potentials. Analytical expressions for the cooling efficiency of C⁺(²P_{1/2}) and Si⁺(²P_{1/2}) are given for the temperature interval 15–2000 K.

Subject headings: ISM: atoms — ISM: molecules — scattering

1. INTRODUCTION

Fine-structure excitations of atoms and ions in collisions with atomic hydrogen provide the dominant cooling mechanisms of diffuse interstellar clouds at low temperatures (Dalgarno & Rudge 1964; Dalgarno & McCray 1972). Inelastic collisions of carbon and silicon ions with hydrogen atoms are especially important due to high abundances of these ions. The open-shell structure of the hydrogen atom and the ions leads to strong interactions, and the binding energies of the CH⁺ and SiH⁺ molecules are large. Many partial waves contribute to the cross sections for C⁺-H and Si⁺-H scattering, and the collision complex may be trapped in shape and Feshbach resonances. The collision complex may emit a photon, thereby forming a stable molecule through radiative association, or it can decay back into the fragments leading to an elastic or inelastic collision.

The cross sections for inelastic collisions of carbon ions with hydrogen, C⁺(²P_{1/2}) + H → C⁺(²P_{3/2}) + H, have been calculated by Wofsy et al. (1971) and Launay & Roueff (1977), and for collisions of silicon ions with hydrogen, Si⁺(²P_{1/2}) + H → Si⁺(²P_{3/2}) + H, by Roueff (1990). These calculations employed the best available ab initio interaction potentials. However, because of computational restrictions, the potentials underestimated the dissociation energy for some states by up to 50% in comparison with experimental measurements (Helm et al. 1982; Carlson et al. 1980), and the calculated equilibrium distances (*R*_{eq}) of the molecules were too large. For example, *R*_{eq} for the ¹Π state of SiH⁺ was 4.7 a.u., compared to the measured *R*_{eq} = 3.536 a.u. (Douglas & Lutz 1970). The uncertainties of the potentials were larger than the collision energies at low temperatures (10–1000 K). In addition, fine-structure excitation rates at low temperatures are affected by scattering resonances that are sensitive to details of the interaction potentials. No further calculations of the fine-structure relaxation rates for C⁺ and Si⁺ have been reported after the work of Launay & Roueff (1977). In this paper we explore the sensitivity of the fine-structure excitation cross section to details of the interaction potentials, and we calculate the rate coefficients for fine-structure excitation in C⁺-H and Si⁺-H collisions over a wide range of temperatures. We also

examine the dynamics of ion-atom collisions at ultralow collision energies (10^{−9}–1 K) at which elastic and inelastic scattering may be characterized by threshold laws. Several studies of neutral atom collisions at subkelvin temperatures have been carried out, but this is the first calculation of ion-atom collisions at ultralow kinetic energies other than an investigation of rotational quenching of molecular ions by closed-shell atoms (Bodo et al. 2002).

2. POTENTIAL ENERGY CURVES

The interaction of the hydrogen atom in the ²S state with an ion in the ²P state, such as C⁺ or Si⁺, gives rise to four molecular states of ¹Σ⁺, ¹Π, ³Σ⁺, and ³Π symmetries. The spin-orbit interaction and rotational coupling split these four states into 12 states. At large interatomic distances these states separate into two manifolds of states corresponding to the spin-orbit split ²P_{3/2} and ²P_{1/2} terms of the C⁺ or Si⁺ ion.

Experiments on CH⁺ and SiH⁺ include spectroscopy of the singlet states (Carlson et al. 1980; Sarre et al. 1989; Carrington & Softley 1986) and the study of Feshbach resonances just above the dissociation threshold (Hechtfisher et al. 2002). Theoretical analysis of the CH⁺ absorption cross section (Carrington & Softley 1986; Williams & Freed 1986; Hechtfisher et al. 2002) showed that the resonances arise as a result of the breakdown of the Born-Oppenheimer approximation. In order to reproduce quantitatively the experimental results and identify the resonances, the potential energy curves had to be drastically modified (Hechtfisher et al. 2002). Apparently high-precision ab initio results did not provide interaction potentials that accurately describe the resonances in the spectrum just above the dissociation limit. We found that including electronic core correlation and relativistic effects in the potential energy calculations for CH⁺ gives the dissociation energies and vertical excitation frequencies within 50 cm^{−1} of the experimental data (Barinovš & van Hemert 2004). The positions of the resonances in the photodissociation spectrum computed with these potentials differ by only a few wavenumbers from the experimental results for excitation by radiation at 30,000 cm^{−1}, and the relative

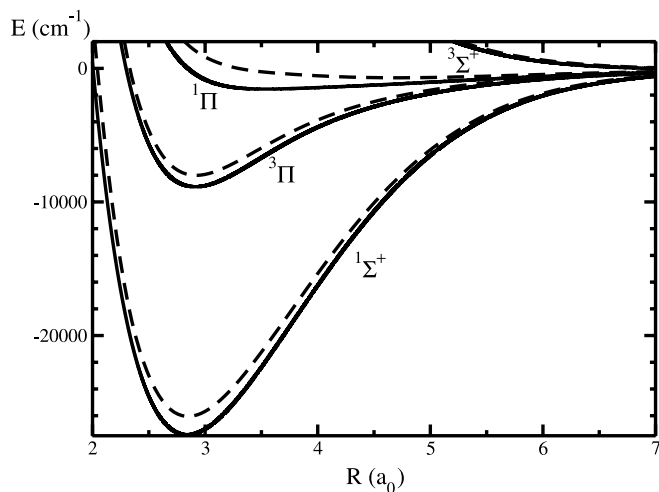


FIG. 1.—Ab initio electronic potentials for SiH^+ . The solid curves show the potentials used in the present calculation, and the dashed curves show the potentials of Hirst (1986).

magnitudes of the resonances are close to the measured values (Hechtfisher et al. 2002). Compared to the potentials used in the previous calculation of fine-structure excitation by Launay & Roueff (1977), our $^1\Sigma^+$, $^1\Pi$, and $^3\Pi$ potentials are about 2000 cm^{-1} deeper, which is about 5% of the depth for the $^1\Sigma^+$ and $^3\Pi$ states and 25% for the $^1\Pi$ state.

The long-range part of an ion-neutral atom potential is determined by the polarization interaction resulting in a strong attraction at large separation. Therefore, we compute the ab initio interaction potentials for the CH^+ (Barinovs & van Hemert 2004) and SiH^+ molecules over a wide range of interatomic distances. The details of the CH^+ potential calculations are given elsewhere (Barinovs & van Hemert 2004). The interaction potentials for the SiH^+ molecule were computed using the same method as that for CH^+ but with a smaller basis set. In order to correlate properly the inner-shell electrons and describe the interaction energy at large distances, the basis sets cc-pCV5Z and aug-pCV5Z were combined to construct the basis set for silicon. The aug-cc-pVQZ basis was used for hydrogen. The Douglas-Kroll relativistic correction was calculated using state-averaged CASSCF with inner shells doubly occupied, followed by a configuration interaction (CI) calculation. In the CI calculation, both the first shell and the second shell were doubly occupied. Calculations were carried out with the MOLPRO package of programs (Werner et al. 2003).

Figure 1 presents a comparison of our potentials for SiH^+ with those of Hirst (1986). The potentials we obtained are in better agreement with the experimental data. For the $^1\Pi$ state the calculated equilibrium distance is $r_{\text{eq}} = 3.538 \text{ a.u.}$, compared to the experimental value $r_{\text{eq}} = 3.536 \text{ a.u.}$ (Douglas & Lutz 1970), and the calculated value of the dissociation energy is $D_0 = 1180 \text{ cm}^{-1}$ compared to the well depth $D_e = 733 \text{ cm}^{-1}$ of the potential of Hirst (1986) and the experimental value of $D_0 = 1230 \pm 210 \text{ cm}^{-1}$. Our calculation of the $^1\Pi$ potential yields the vibrational frequencies corresponding to $\Delta G_{1/2} = 359.6 \text{ cm}^{-1}$ whereas the experimental $\Delta G_{1/2} = 388.67 \text{ cm}^{-1}$ (Carlson et al. 1980).

3. DYNAMICAL CALCULATIONS

The method of our scattering calculations is based on the work of Reid & Dalgarno (1969), Mies (1973), Reid (1973), and Krems et al. (2004). The total Hamiltonian of the $\text{C}^+(^2P)$ -

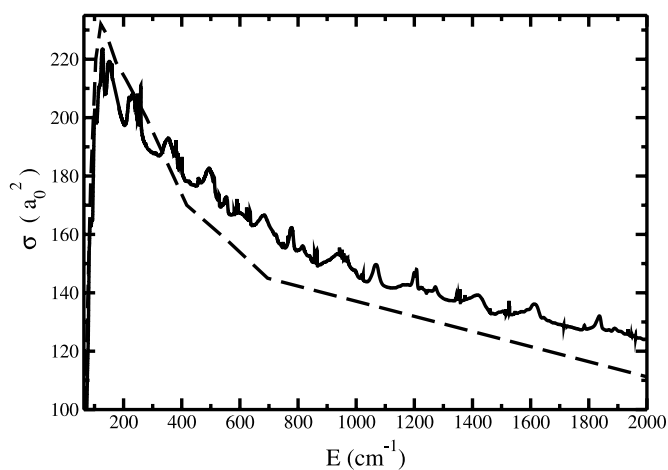


FIG. 2.—Excitation cross sections for the $\text{C}^+(^2P_{1/2}) + \text{H} \rightarrow \text{C}^+(^2P_{3/2}) + \text{H}$ reaction. The solid curve represents the results of the present calculation, and the dashed curve represents the results of Launay & Roueff (1977).

$\text{H}(^2S)$ or $\text{Si}^+(^2P)$ - $\text{H}(^2S)$ system can be written in atomic units in the form

$$\hat{H} = -\frac{1}{2\mu R} \frac{\partial^2}{\partial R^2} R + \frac{l^2}{2\mu R^2} + \hat{V}_{\text{el}} + \hat{V}_{\text{so}}, \quad (1)$$

where R is the interatomic distance, l is the angular momentum describing the rotation of the vector \mathbf{R} , \hat{V}_{el} is the electrostatic interaction potential between the ion and the hydrogen atom, and \hat{V}_{so} is the operator describing the spin-orbit interaction in the ion. We have neglected the interatomic magnetic dipole interaction. The total wave function ψ^{JM} , corresponding to a given value of the total angular momentum J and its space-fixed projection M , is represented by a close coupling expansion,

$$\psi^{JM} = \sum_l \sum_j \sum_{j_A} F_{jlj_H j_A}^{JM}(R) |JMjlj_H j_A\rangle, \quad (2)$$

with the function $|JMjlj_H j_A\rangle$ defined in the Appendix.

Substitution of expansion (2) in Schrödinger's equation results in a system of coupled differential equations,

$$\left[\frac{d^2}{dR^2} - \frac{l(l+1)}{R^2} + 2\mu E \right] F_{jlj_H j_A}^J(R) = 2\mu \sum_{j'l'_A} U_{jlj_H j_A; j'l'_A}^J F_{j'l'_A}^{Jj'_A}(R), \quad (3)$$

with the coupling matrix U given by the sum of the matrices $V_{\text{el}} + V_{\text{so}}$ in the basis of equation (2). The matrix U is independent of M , so the subscript M has been omitted from equation (3).

The matrix of the spin-orbit interaction operator \hat{V}_{so} is diagonal in the basis $|JMjlj_H j_A\rangle$ with the matrix elements Δ_{j_A} corresponding to the asymptotic energies of the ion,

$$\langle JMjlj_H j_A | \hat{V}_{\text{so}} | JMj'l'_A j'_A \rangle = \delta_{jj'} \delta_{ll'} \delta_{j_A j'_A} \Delta_{j_A}. \quad (4)$$

We adopt $\Delta_{j_A=1/2} = 0$ for both ions, $\Delta_{j_A=3/2} = 63.42 \text{ cm}^{-1}$ for the carbon ion, and $\Delta_{j_A=3/2} = 287 \text{ cm}^{-1}$ for the silicon ion. In order to evaluate the matrix of the electronic interaction potential \hat{V}_{el} , we use the formalism described by Krems et al. (2004). Explicit expressions for the matrix elements are given in the Appendix. The solution of the close coupled equation (3) at a fixed total energy E with the scattering boundary conditions

TABLE 1
THE CALCULATED COOLING EFFICIENCIES $L(T)$ AND QUENCHING RATE COEFFICIENTS $Q(T)$

T (K)	L (10^{-24} ergs $\text{cm}^3 \text{s}^{-1}$)		Q (10^{-10} $\text{cm}^3 \text{s}^{-1}$)	
	$\text{C}^+(^2P_{1/2 \rightarrow 3/2})$	$\text{Si}^+(^2P_{1/2 \rightarrow 3/2})$	$\text{C}^+(^2P_{3/2 \rightarrow 1/2})$	$\text{Si}^+(^2P_{3/2 \rightarrow 1/2})$
20.....	0.16	0.00	5.96	4.52
40.....	1.75	0.00	6.79	4.83
60.....	3.96	0.06	7.19	5.04
80.....	5.97	0.34	7.42	5.22
100.....	7.67	0.99	7.58	5.39
120.....	9.09	2.03	7.72	5.55
140.....	10.29	3.40	7.84	5.70
160.....	11.33	5.04	7.96	5.84
180.....	12.24	6.87	8.06	5.98
200.....	13.04	8.83	8.17	6.10
300.....	16.04	19.17	8.63	6.66
400.....	18.09	28.92	9.02	7.12
600.....	20.92	45.30	9.67	7.91
800.....	22.93	58.38	10.20	8.58
1000.....	24.51	69.23	10.66	9.17
1500.....	27.45	90.80	11.58	10.49
2000.....	29.63	108.92	12.31	11.74

(Arthurs & Dalgarno 1960) yields the scattering S -matrix from which the cross sections and rate coefficients for inelastic collisions can be computed using standard relations.

4. RESULTS

Figure 2 presents the cross section $\sigma(E)$ for the excitation of $\text{C}^+(^2P_{1/2})$ as a function of the collision energy. Our calculation gives a larger cross section than that of Launay & Roueff (1977) at collision energies above 300 cm^{-1} . The energy dependence of the cross section shows many resonance peaks that were not observed by Launay & Roueff because of the sparse energy grid they used. The peaks in the cross section are due to shape resonances. Feshbach resonances occur at energies lower than the energy of the spin-orbit splitting and would be apparent in the elastic cross sections.

The cooling efficiency for the excitation is given by

$$L(T) = \Delta_{3/2}R(T),$$

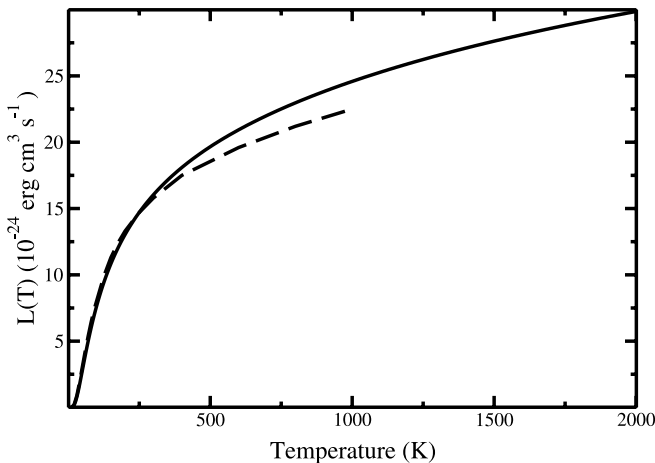


FIG. 3.—Cooling efficiency for $\text{C}^+(^2P_{1/2})$ in collisions with hydrogen. The solid curve represents the results of the present calculation, and the dashed curve represents the results of Launay & Roueff (1977).

where $R(T)$ is the excitation rate coefficient,

$$R(T) = \left(\frac{8kT}{\pi\mu}\right)^{1/2} \frac{1}{(kT)^2} \int \sigma(E)E \exp\left(\frac{-E}{kT}\right) dE.$$

Values of $L(T)$ for temperatures up to 2000 K are listed in Table 1 and compared in Figure 3 with the results of Launay & Roueff (1977). At low temperatures the two calculations agree well, but above 300 K we obtain a higher cooling efficiency.

In Figure 4 we compare the cross sections for the $\text{Si}^+(^2P_{1/2}) \rightarrow \text{Si}^+(^2P_{3/2})$ excitation with those of Roueff (1990). The cooling efficiencies are listed in Table 1 and compared in Figure 5 with the results of Roueff (1990). Our cooling efficiencies are about 10% higher.

The cooling efficiencies may be represented as functions of temperature by the expressions

$$L(T) = \exp(-91.2/T)(16 + 0.344\sqrt{T} - 47.7/T) \times 10^{-24} \text{ ergs cm}^3 \text{ s}^{-1}$$

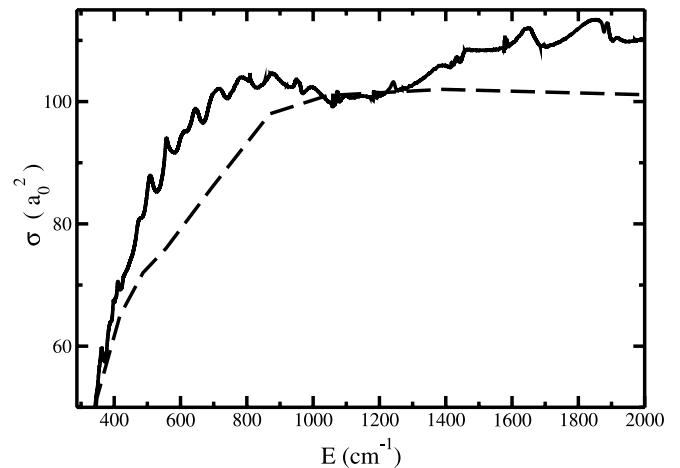


FIG. 4.—Excitation cross sections for the $\text{Si}^+(^2P_{1/2}) + \text{H} \rightarrow \text{Si}^+(^2P_{3/2}) + \text{H}$ reaction. The solid curve represents the results of the present calculation, and the dashed curve represents the results of Roueff (1990).

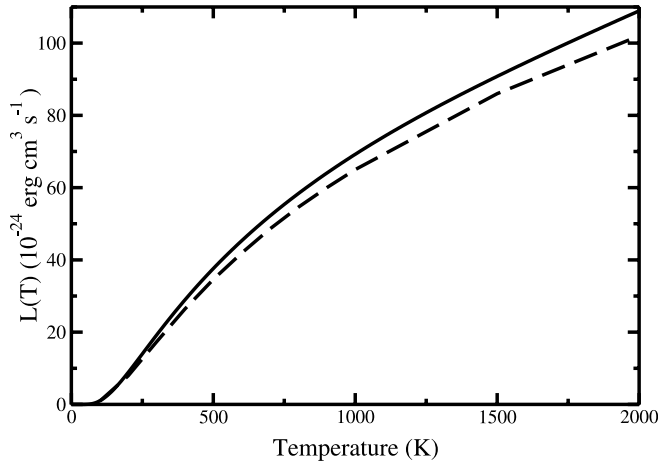


FIG. 5.—Cooling efficiency for $\text{Si}^+(^2P_{1/2})$ in collisions with hydrogen. The solid curve represents the present results, and the dashed curve represents the results of Roueff (1990).

for the $\text{C}^+(^2P_{1/2}) \rightarrow \text{C}^+(^2P_{3/2})$ excitation and

$$L(T) = \exp(-413/T)(43.5 + 1.78\sqrt{T} + 0.005T) \times 10^{-24} \text{ erg cm}^3 \text{ s}^{-1}$$

for the $\text{Si}^+(^2P_{1/2}) \rightarrow \text{Si}^+(^2P_{3/2})$ excitation. The analytical expressions reproduce the calculated cooling rate coefficients with a relative deviation within 1% at temperatures between 15 and 2000 K. The excitation rate coefficients can be found as

$$R(T) = 7.938 \times 10^{13} L(T) \text{ cm}^3 \text{ s}^{-1}$$

for the $\text{C}^+(^2P_{1/2}) \rightarrow \text{C}^+(^2P_{3/2})$ transition and

$$R(T) = 1.75 \times 10^{13} L(T) \text{ cm}^3 \text{ s}^{-1}$$

for the $\text{Si}^+(^2P_{1/2}) \rightarrow \text{Si}^+(^2P_{3/2})$ transition. The temperature-dependent quenching rate coefficients $Q(T)$ for the $\text{C}^+(^2P_{3/2}) \rightarrow \text{C}^+(^2P_{1/2})$ and $\text{Si}^+(^2P_{3/2}) \rightarrow \text{Si}^+(^2P_{1/2})$ de-excitation can be obtained from the excitation rate coefficients as

$$Q(T) = \frac{1}{2} e^{\Delta_{3/2}/kT} R(T).$$

Values of $Q(T)$ are listed in Table 1.

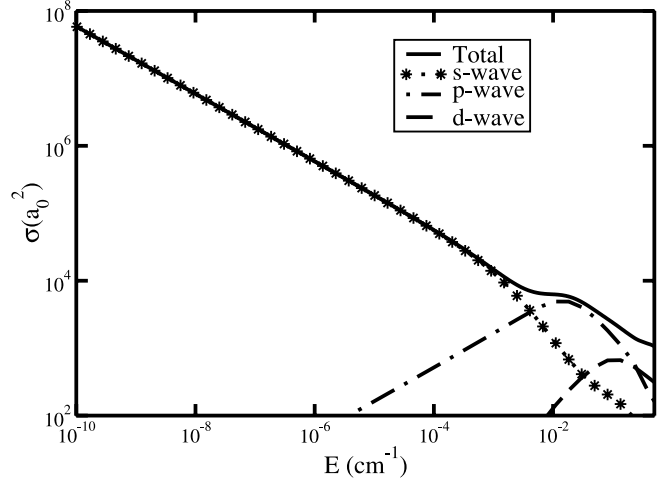


FIG. 6.—Low-energy de-excitation cross sections for $\text{C}^+(^2P_{3/2}) + \text{H} \rightarrow \text{C}^+(^2P_{1/2}) + \text{H}$ as functions of the kinetic energy.

Because of the widespread interest in scattering processes in ultracold gases, we extended our study of C^+ -H collisions to zero energy. Figure 6 depicts the individual partial-wave contributions to the total cross section for fine-structure relaxation of $\text{C}^+(^2P_{3/2})$ in the energy interval between 10^{-10} and 10^{-1} cm^{-1} . The cross sections follow the Wigner threshold law (Wigner 1948; Krens 2002) for inelastic scattering. The s-wave cross section is inversely proportional to the collision velocity at energies less than 10^{-3} cm^{-1} , yielding a finite zero temperature rate coefficient of $2.6 \times 10^{-10} \text{ cm}^3 \text{ s}^{-1}$. The higher partial waves contribute to the cross section at collision energies above $5 \times 10^{-3} \text{ cm}^{-1}$ and eventually dominate.

This work was supported by the National Science Foundation through a grant for the Institute for Theoretical Atomic and Molecular Physics at the Smithsonian Astrophysical Observatory and Harvard University; by the Chemical Sciences, Geosciences and Biosciences Division, Office of Basic Energy Sciences, Office of Science, US Department of Energy; and by the Nederlandse Organisatie voor Wetenschappelijk Onderzoek (NWO). R. K. is supported by the Harvard-MIT Center for Ultracold Atoms.

APPENDIX

The total wavefunction in equation (2) is expressed as

$$\begin{aligned} |JMjlj_{\text{H}}j_{\text{A}}\rangle &= \sum_{M_{L_{\text{H}}}} \sum_{M_{S_{\text{H}}}} \sum_{M_{L_{\text{A}}}} \sum_{M_{S_{\text{A}}}} \sum_{m_{j_{\text{H}}}} \sum_{m_{j_{\text{A}}}} \sum_{m_j} \sum_{m_l} |L_{\text{H}}M_{L_{\text{H}}}\rangle |S_{\text{H}}M_{S_{\text{H}}}\rangle |L_{\text{A}}M_{L_{\text{A}}}\rangle |S_{\text{A}}M_{S_{\text{A}}}\rangle |lm_l\rangle \\ &\times \langle L_{\text{H}}M_{L_{\text{H}}}S_{\text{H}}M_{S_{\text{H}}}|j_{\text{H}}m_{j_{\text{H}}}\rangle \langle L_{\text{A}}M_{L_{\text{A}}}S_{\text{A}}M_{S_{\text{A}}}|j_{\text{A}}m_{j_{\text{A}}}\rangle \langle j_{\text{H}}m_{j_{\text{H}}}j_{\text{A}}m_{j_{\text{A}}}|jm_j\rangle \langle jm_jlm_l|JM\rangle, \end{aligned} \quad (\text{A1})$$

where L_{H} and L_{A} are the electronic orbital angular momenta, S_{H} and S_{A} are the electronic spin angular momenta, and j_{H} and j_{A} are the total electronic angular momenta of the hydrogen atom (subscript H) and the ion (subscript A). The vector sum of j_{H} and j_{A} determines the total electronic angular momentum of the diatomic system j . The projections of the corresponding angular momenta on the space-fixed quantization axis are represented by $M_{L_{\text{H}}}$, $M_{L_{\text{A}}}$, $m_{j_{\text{H}}}$, $m_{j_{\text{A}}}$, m_j , and m_l . The electronic orbital angular momentum L_{H} of the ground-state hydrogen is zero, so that $j_{\text{H}} = S_{\text{H}} = 1/2$ and there is no spin-orbit interaction in the hydrogen atom in first order.

The electronic interaction potential between two arbitrary atoms can be represented in an effective potential form as

$$\hat{V}_{\text{el}} = \sum_S \sum_{M_S} |SM_S\rangle \langle SM_S| \hat{V}^S, \quad (\text{A2})$$

with \hat{V}^S given by

$$\hat{V}^S = (4\pi)^{1/2} \sum_{k_1} \sum_{k_2} \sum_k V_{k_1, k_2, k}^S(R) \sum_{q_1} \sum_{q_2} \sum_q (-1)^{k_1 - k_2} \begin{pmatrix} k_1 & k_2 & k \\ q_1 & q_2 & q \end{pmatrix} \hat{T}_{q_1}^{k_1}(L_H) \hat{T}_{q_2}^{k_2}(L_A) Y_{kq}(\hat{R}), \quad (\text{A3})$$

where $\hat{T}_{q_1}^{k_1}(L_H)$ and $\hat{T}_{q_2}^{k_2}(L_A)$ are the spherical tensors defined in Krems et al. (2004), the symbol in parentheses is a $3j$ symbol, and the expansion coefficients $V_{k_1, k_2, k}^S(R)$ can be expressed in terms of the Born-Oppenheimer potentials $V_{\Lambda}^S(R)$ for atom-atom interactions as

$$V_{k_1, k_2, k}^S(R) = \sum_L \sum_{L'} \sum_{\Lambda} V_{\Lambda}^S(R) (-1)^{L-\Lambda} \begin{pmatrix} L & k & L \\ -\Lambda & 0 & \Lambda \end{pmatrix} [(k_1)(k_2)(k)(L)(L)]^{1/2} \left\{ \begin{matrix} L_H & L_H & k_1 \\ L_A & L_A & k_2 \\ L & L & k \end{matrix} \right\}. \quad (\text{A4})$$

The symbol in curly braces is a $9j$ symbol, $L = L_A$, Λ is the projection of L on the interatomic distance, and the shorthand notation (L) is used for $(2L + 1)$. For the C⁺(²P)–H(²S) and Si⁺(²P)–H(²S) systems, equation (A4) reduces to two nonzero terms, $V_{0,0,0}^S(R) = [V_{\Sigma}^S(R) + 2V_{\Pi}^S(R)]/\sqrt{3}$ and $V_{0,2,2}^S(R) = [-V_{\Sigma}^S(R) + V_{\Pi}^S(R)](2/3)^{1/2}$. Using equations (A2), (A3), and (A4), we evaluate the matrix elements of the interaction potential \hat{V}_{el} in the basis of equation (2). They have the form

$$\begin{aligned} \langle JMj l j_A j_B | \hat{V}_{\text{el}} | JMj' l' j_A j_B \rangle &= \sum_S \sum_{k_1} \sum_{k_2} \sum_k V_{k_1, k_2, k}^S(R) \sum_f \sum_{f'} \begin{pmatrix} l & k & l' \\ 0 & 0 & 0 \end{pmatrix} \\ &\times [(j_H)(j'_H)(j_A)(j'_A)(j)(j')(l)(l')(S)^2(k_1)(k_2)(k)(f)^2(f')^2]^{1/2} (-1)^{f+k+J-S} \\ &\times \left\{ \begin{matrix} L_H & S_H & j_H \\ L_A & S_A & j_A \\ f & S & j \end{matrix} \right\} \left\{ \begin{matrix} L_H & S_H & j_H \\ L_A & S_A & j'_A \\ f' & S & j' \end{matrix} \right\} \left\{ \begin{matrix} L_H & L_H & k_1 \\ L_A & L_A & k_2 \\ f & f' & k \end{matrix} \right\} \left\{ \begin{matrix} j & j' & k \\ l' & l & J \end{matrix} \right\} \left\{ \begin{matrix} j & j' & k \\ f' & f & S \end{matrix} \right\}. \quad (\text{A5}) \end{aligned}$$

REFERENCES

- Arthurs, A. M., & Dalgarno, A. 1960, Proc. R. Soc. London A, 256, 540
 Barinovs, Ģ., & van Hemert, M. C. 2004, Chem. Phys. Lett., 399, 406
 Bodo, E., Scifoni, E., Sebastianelli, F., Gianturco, F. A., & Dalgarno, A. 2002, Phys. Rev. Lett., 89, 283201
 Carlsson, T. A., Copley, J., Duric, N., Elander, N., Erman, P., Larson, M., & Lyrra, M. 1980, A&A, 83, 238
 Carrington, A., & Softley, T. P. 1986, Chem. Phys., 106, 315
 Dalgarno, A., & McCray, R. A. 1972, ARA&A, 10, 375
 Dalgarno, A., & Rudge, M. R. H. 1964, ApJ, 140, 800
 Douglas, A. E., & Lutz, B. L. 1970, Canadian J. Phys., 48, 247
 Hechtfisher, U., Williams, C. J., Lange, M., Linkemann, J., Schwalm, D., Wester, R., Wolf, A., & Zajfman, D. 2002, J. Chem. Phys., 117, 8754
 Helm, H., Cosby, P. C., Graff, M. M., & Moseley, J. T. 1982, Phys. Rev. A, 25, 304
 Hirst, D. M. 1986, Chem. Phys. Lett., 128, 504
 Krems, R. V. 2002, Recent Res. Dev. Chem. Phys., 3, 485
 Krems, R. V., Groenenboom, G. C., & Dalgarno, A. 2004, J. Phys. Chem. A, 108, 8941
 Launay, J.-M., & Roueff, E. 1977, J. Phys. B, 10, 879
 Mies, F. H. 1973, Phys. Rev. A, 7, 942
 Reid, R. H. G. 1973, J. Phys. B, 6, 2018
 Reid, R. H. G., & Dalgarno, A. 1969, Phys. Rev. Lett., 22, 1029
 Roueff, E. 1990, A&A, 234, 567
 Sarre, P. J., Whitham, C. J., & Graff, M. M. 1989, J. Chem. Phys., 90, 6061
 Werner, H.-J., et al. 2003, MOLPRO 2002.6 (Birmingham: Univ. Birmingham), <http://www.molpro.net>
 Wigner, E. P. 1948, Phys. Rev., 73, 1002
 Williams, C. J., & Freed, K. F. 1986, J. Chem. Phys., 85, 2699
 Wofsy, S., Reid, R. H. G., & Dalgarno, A. 1971, ApJ, 168, 161